Organic & Biomolecular Chemistry

Accepted Manuscript

This article can be cited before page numbers have been issued, to do this please use: X. Zeng, Q. Wang, K. Huang, S. Cai, C. Liu, X. Jiao, S. He and L. Zhao, *Org. Biomol. Chem.*, 2018, DOI: 10.1039/C8OB01701H.

ROYAL SOCIETY OF CHEMISTRY

rsc.li/obc

View Article Online
DOI: 10.1039/C8OB01701H

Journal Name

ARTICLE

Synthesis of Near-Infrared Fluorescent Rhodamines via an S_NAr^H Reaction and Their Biological Applications

Received 00th January 20xx,
Accepted 00th January 20xx

DOI: 10.1039/x0xx00000x

www.rsc.org/

Qing Wang,[ab] Kun Huang,[a] Songtao Cai,[b] Chang Liu,[a] Xiaojie Jiao,[a] Song He,[a] Liancheng Zhao,[b] and Xianshun Zeng*[ab]

Near-infrared (NIR) dyes are of great interest in biomedicine due to diminished interfering absorption and fluorescence from biological samples, reduced scattering, and enhanced tissue penetration depth. In this context, we report the synthesis of rectilinearly π-extended rhodamine dyes using a unique intramolecular nucleophilic substitution of aromatic hydrogen (S_NAr^H) strategy. The strategy makes use of an S_NAr^H reaction between a preorganized aromatic amino nitrogen and an electron-deficient carbon in the xanthylium ion. The S_NAr^H reaction presented herein can be performed under mild conditions without a transition metal catalyst and can be expected to enable the preparation of a wide variety of π-extended near-infrared fluorescent rhodamine dyes. Using this strategy, seven rectilinearly π-extended rhodamines (**RE1–RE7)** that had fluorescence emission wavelengths in the near-infrared region were synthesized. **RE1**, **RE3**, and **RE4** were lysosome targetable and showed good photostabilities. In addition, using dye **RE1** as a precursor, we constructed a novel NIR fluorescent turn-on probe (**RE1-Cu**), which can be used for detecting Cu^{2+} in living cells, demonstrating the value of our NIR functional fluorescent dyes.

Introduction

Considerable effort has been expended towards the development of fluorescent-probe-based imaging techniques, which are powerful, noninvasive tools for visualization of biological processes and which have potential clinical applications.[1] However, the performance of the probes depends strongly on their photophysical properties. Various fluorescent dyes have been used for designing probes.[2] It has been reported that the use of near-infrared (NIR) fluorescence imaging (λ_{em} > 650 nm) techniques can minimize photodamage to living samples, increase tissue penetration depth, and minimize interference due to autofluorescence.[3] The most widely used NIR dyes for such purposes are cyanine dyes, such as Cy5 and Cy7.[4] However, these dyes have some drawbacks for biological imaging; for example, they often suffer from photobleaching, low quantum yields, and narrow Stokes shifts.[5]

Recently, Qian, Nagano, and co-workers synthesized Si-rhodamines, in which the bridging oxygen atom in the xanthene moiety is replaced with a silicon atom and which have emission wavelengths in the NIR region (λ_{em} > 660 nm).[6] The development of these probes was an important milestone in NIR fluorescence bioimaging. Si-rhodamines possess all the favorable characteristics of traditional rhodamines, and a number of excellent rationally designed Si-rhodamine probes have been synthesized for NIR imaging.[7] Extending the π-conjugation of the xanthene moiety by adding aromatic rings has also been shown to be a versatile strategy for red-shifting the excitation and emission bands of xanthene dyes. For example, Strongin et al. synthesized ring-expanded seminaphthofluorones that exhibit clearly red-shifted absorption and emission maxima.[8] Other angular π-expanded xanthenes, such as seminaphthorhodamine,[9] also show fluorescence emission that is significantly red-shifted (into NIR region).

Herein, we reported the synthesis of rectilinearly π-extended NIR fluorescent rhodamines via an intramolecular nucleophilic substitution of aromatic hydrogen (S_NAr^H) reaction [10] under mild metal-free conditions (Scheme 1a). Most of the widely used methods for constructing C–N bond involve transition metal catalysis.[11] However, these methods generally require harsh reaction conditions or generate metal waste, and these features limit their applications.[11d] Metal-free S_NAr^H reactions offer an potential alternative approach for constructing C–N bonds,[10] but reported examples of metal-free S_NAr^H reactions for constructing C–N bond that can be conducted under mild conditions are limited in number.[12] In this study, we synthesized seven dyes **RE1**–**RE7** (Scheme 1b) by fusing an aromatic ring directly to the xanthene scaffold of rhodamine via a metal-free intramolecular S_NAr^H reaction. The

[a] Tianjin Key Laboratory for Photoelectric Materials and Devices, Department of Function Materials, School of Materials Science and Engineering, Tianjin University of Technology, Tianjin 300384, China. E-mail: xshzeng@tjut.edu.cn.
[b] School of Materials Science and Engineering, Harbin Institute of Technology, Harbin 150001, China.

†Electronic Supplementary Information (ESI) available: Experimental details, characterization data for new compounds; additional schemes, figures; copies of NMR spectra; HRMS spectra (PDF); X-ray crystallographic file of dye **RE1** (CIF); videos S1-S4 (AVI). See DOI: 10.1039/x0xx00000x

View Article Online
DOI: 10.1039/C8OB01701H

emission maxima of **RE1**–**RE7** were significantly red-shifted (to the NIR region) compared to the corresponding emission maxima of traditional rhodamine dyes. Dyes **RE1**, **RE3** and **RE4** are highly lysosome targetable and exhibit clear fluorescence signals in living cells without any background interferences. In order to demonstrate the value of our dyes for probe design, a probe, **RE1-Cu** for Cu^{2+} was synthesized and applied for imaging of Cu^{2+} in living cells.

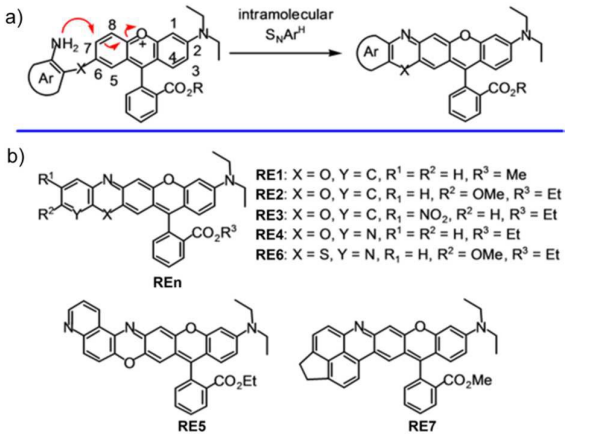

Scheme 1 a) Retrosynthetic analysis of rectilinearly π-extended rhodamines **RE1–RE6** and b) structures of **RE1–RE7**.

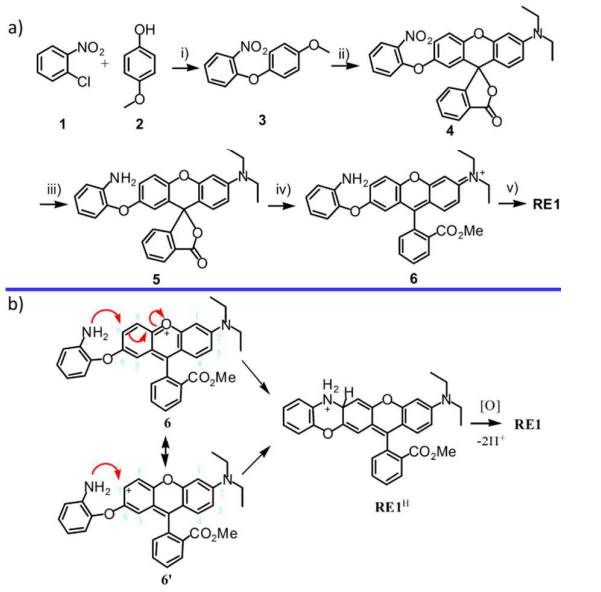

Scheme 2 a) Synthesis of **RE1**. b) Proposed mechanism of the S_NAr^H reaction of **6** to form **RE1**. Reagents and conditions: (i) DMF, Na_2CO_3, 100 °C. (ii) 2-(4-(*N*,*N*-diethylamino)-2-hydroxybenzoyl)benzoic acid, CH_3SO_3H, 85 °C. (iii) $SnCl_2$, EtOH, 85 °C. (iv) MeOH, H_2SO_4 (98 wt%), reflux. (v) Na_2CO_3, EtOAc, 50 °C. (vi) Na_2CO_3, toluene, 110 °C.

Results and discussion

Design and synthesis of π-extended rhodamine dyes RE1-RE7

Both computational and experimental studies[10] have demonstrated that the critical factor for the success of an S_NAr^H reaction is that the aromatic carbon center attacked by the nucleophile must be sufficiently electron deficient to favor the formation of a transient σ^H adduct, which undergoes subsequent oxidation to yield the C–N linking product. Therefore, we began by synthesizing xanthylium ion intermediate **6**, which has an electron-deficient carbon at the 7-position of the xanthene moiety and which we expected would efficiently form the transient σ^H adduct necessary for the synthesis of **RE1** (Scheme 2b). Specifically, an S_NAr^X reaction of 2-chloronitrobenzene (**1**) and 4-methoxylphenol (**2**) afforded intermediate **3** (Scheme 2a). Condensation of **3** with 2-(4-(*N*,*N*-diethylamino)-2-hydroxybenzoyl)benzoic acid in CH_3SO_3H afforded rhodamine analogue **4** through Friedel–Crafts type reactions (Scheme S10).[2f, 26] Then **4** was reduced with $SnCl_2{\cdot}2H_2O$ in ethanol to afford amine **5**, which was refluxed in methanol in the presence of concentrated H_2SO_4 to afford the key xanthylium ion (**6**). Finally, the rectilinearly π-extended rhodamine dye **RE1** was obtained in 52% yield by intramolecular S_NAr^H reaction of **6** under basic conditions (Na_2CO_3) at 50 °C (Schemes 2a and S1). It is noteworthy that a solution of **6** in DMF underwent spontaneously conversion to **RE1** at room temperature within a few days in the absence of any base, which indicated that the S_NAr^H reaction could occur under mild conditions.

A proposed mechanism for the critical intramolecular S_NAr^H annulation of **6** to form **RE1** is shown in Scheme 2b. In addition to the ammonium ion form,[2c] compound **6** has two other resonance structures: oxonium ion **6** and transient carbocation **6'**. The oxonium ion and carbocation structures are favorable for the intramolecular S_NAr^H reaction at the highly electron-deficient C-7. From **6**, the S_NAr^H reaction can proceed via a Michael-type addition of the amino nitrogen atom to C-7 to form a six-membered-ring transient σ^H adduct **RE1^H**. From **6'**, the S_NAr^H reaction can proceed via addition of the nitrogen atom to the transient carbocation at the 7-position to form **RE1^H**. Then **RE1^H** is converted to **RE1** via spontaneous oxidation to yield the C–N linking product.[15] It is noteworthy that amine **5** did not undergo the annulation reaction even at elevated temperature (110 °C) in toluene, mainly because **5** exists in a spirolactone structure under neutral and basic conditions in organic solvents. This result implies that the intramolecular S_NAr^H annulation reaction of **6** was driven primarily by electronic effects, that is, by the electron deficiency at C-7.

To evaluate the feasibility of this S_NAr^H annulation strategy, we considered a number of factors that might influence the S_NAr^H annulation reaction, such as electronic effects, as well as replacement of the benzene ring with a heterocyclic ring or replacement of the bridging oxygen atom with a sulfur atom or a benzo ring. Specifically, we synthesized rectilinearly π-extended rhodamines **RE2**–**RE7** via the intramolecular S_NAr^H reaction (Schemes 1 and S2–S7). The synthetic strategy mainly includes two critical steps: the synthesis of 2'-aminoaryl linked xanthylium and the intramolecular S_NAr^H reaction to form the rectilinearly π-extended NIR rhodamine dyes. Followed the similar synthesis procedures for the preparation of dye **RE1**,

View Article Online
DOI: 10.1039/C8OB01701H

dyes **RE2**-**RE6** were prepared. For **RE7**, the critical starting materials **35** was synthesized by the Suzuki coupling reaction between 4-bromo-5-nitroacenaphthene **33** and 4-methoxyphenylboronic acid **34**. **RE2** and **RE3** contain an electron-donating methoxyl group and an electron-withdrawing nitro group, respectively. **RE4** and **RE5** are pyridine- and quinoline-fused rhodamines, respectively. In **RE6**, the oxygen atom is replaced with a sulfur atom, and the benzene ring is replaced with a pyridine ring. Different from **RE1**–**RE6**, the acenaphthene moiety in **RE7** is linked to xanthene directly without a linker atom, such as oxygen or sulfur, and the intramolecular S_NAr^H reaction still proceeds smoothly under very mild conditions (Scheme S7). Our successful syntheses of **RE1**–**RE7** confirmed the feasibility of the S_NAr^H C–N annulation strategy for the efficient construction of rectilinearly π-extended rhodamine dyes.

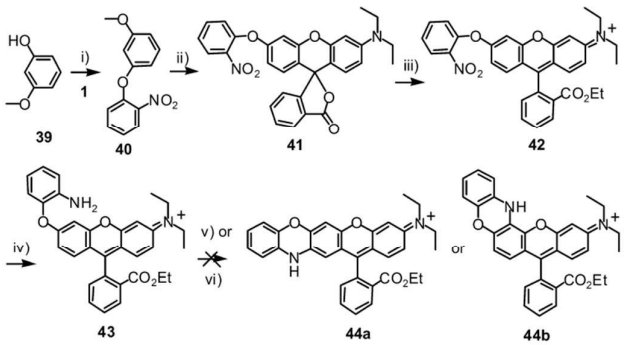

Scheme 3 The control experiment of synthesis of **43**. Reagents and conditions: (i) DMF, Na_2CO_3, 100 °C for 14 h; (ii) 2-(4-(*N*,*N*-diethylamino)-2-hydroxybenzoyl)benzoic acid, CH_3SO_3H, 85 °C for 3 d; (iii) EtOH, H_2SO_4, refluxed for 24 h; (iv) $SnCl_2{\cdot}2H_2O$, EtOH, refluxed for 10 h; (v) Na_2CO_3, EtOAc, 50 °C for 4 h; (vi) Na_2CO_3, toluene, 110 °C for 4 h.

Control experiment

To verify our speculation that the intramolecular S_NAr^H reaction proceeds only at the highly electron-deficient transient carbocation of the xanthylium skeleton, we conducted a control experiment (Schemes 3 and S8). Specifically, we prepared compound **43**, in which the 2'-aminophenoxyl moiety is attached to C-7 of the xanthylium ion, and then we attempted to prepare annulation product **44a** or **44b** by means of the intramolecular S_NAr^H reaction. As expected, the S_NAr^H reaction of **43** did not proceed even at increased temperature (110 °C), because a highly electron-deficient transient carbocation cannot form at either the 6-position or the 8-position.

X-Ray crystal structure analysis of RE1

To confirm the formation of the C–N bond, we obtained a single crystal of **RE1** by slow evaporation of 2:1 (v/v) MeOH/CH_2Cl_2 and subjected it to X-ray crystallographic analysis (Table S1 and Fig. 1). We were encouraged to observe that the amino nitrogen was bonded to C-8 of the xanthene moiety, which is solid evidence for the S_NAr^H annulation. The N1–C8 bond length was 1.3414 Å, which is typical for a C=N bond and is much shorter than the N1–C1 bond length (1.3936 Å); this means that the N1=C8 bond formed after the intramolecular annulation. The formation of the N1=C8 bond contributes to the formation of a coplanar conjugated structure composed of five six-membered rings, namely, three fused benzene rings separated by an oxazine ring and a pyran ring; the structure is analogous to that of pentacene (Fig. 1). The mean plane of the five fused rings was almost orthogonal (dihedral angle 89.10°) to the plane of the benzene ring of the benzoic acid methyl ester group.

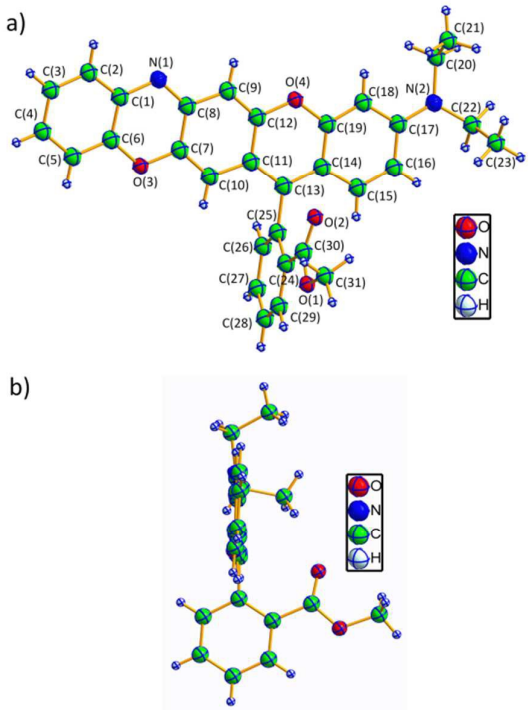

Fig. 1 Single crystal X-ray structure of **RE1**. a) Top view along the xanthylium plane and b) side view along the xanthylium plane.

Optical properties of dyes RE1–RE7

The photophysical properties of **RE1**–**RE7** in ethanol were investigated (Fig. 2 and S1, Table 1). **RE1** showed intense absorption and emission bands at 628 and 680 nm, respectively, the latter representing a large (108 nm) red shift relative to the emission band of rhodamine B (**Rho B**). **RE2**, which has an electron-donating methoxyl group, showed even larger red shifts in the absorption and emission wavelengths (to 649 and 716 nm, respectively). Conversely, introduction of an electron-withdrawing nitro group (**RE3**) induced a clear blue shift relative to **RE1**, as well as a remarkable increase of the fluorescence quantum yield (Φ_f = 0.33, $\lambda_{abs}/\lambda_{em}$ = 604/647 nm). Like **RE3**, the electron-deficient pyridine-fused dye **RE4** also showed blue- shifted spectra relative to those of **RE1** and an increased Φ_f ($\lambda_{abs}/\lambda_{em}$ = 602/665 nm, Φ_f = 0.108). Compared with **RE4**, the pyridine-fused **RE6**, in which the oxygen atom was replaced with a sulfur atom, showed prominent red shifts of both the absorption and the emission wavelengths ($\lambda_{abs}/\lambda_{em}$ = 654/745 nm). Quinoline-fused **RE5** ($\lambda_{abs}/\lambda_{em}$ = 618/721 nm, Φ_f < 3%) and acenaphthene-fused **RE7** ($\lambda_{abs}/\lambda_{em}$ = 677/830 nm, Φ_f < 3%), which have π systems that are even more extended

View Article Online
DOI: 10.1039/C8OB01701H

than that of **RE1**, exhibited remarkably red-shifted absorption and emission wavelengths, but their Φ_f values were diminished. It is noteworthy that all seven of the dyes we synthesized exhibited larger Stokes shifts (43 nm) than that of **Rho B** (19 nm), demonstrating their potential utility for bioimaging applications requiring a high signal-to-noise ratio with enhanced contrast discrimination. The emission maxima of the seven dyes and **Rho B** decreased in the order **RE7** > **RE6** > **RE5** > **RE2** > **RE1** > **RE4** > **RE3** > **Rho B**, suggesting that extending the π-conjugation system, introducing an electron-donating group, or replacing the bridging oxygen atom with sulfur atom could increase the absorption and emission wavelengths.

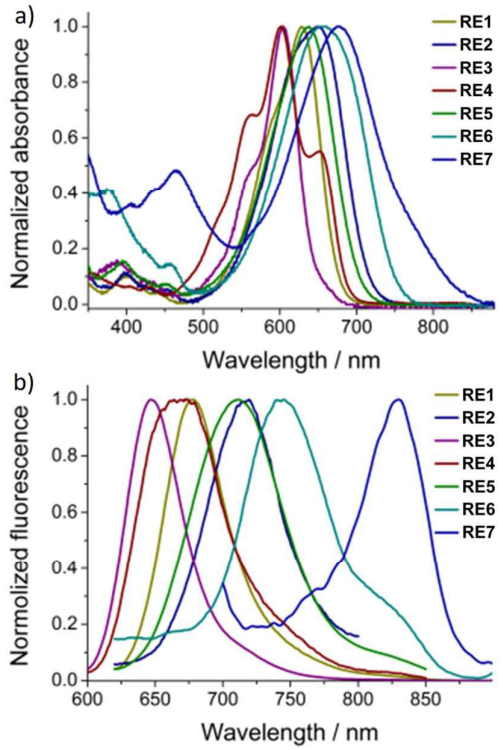

Fig. 2 Normalized UV–vis absorption a) and fluorescence b) spectra of **RE1–RE7** in ethanol.

Table 1 Photophysical properties of rhodamine B (Rho B) and **RE1–RE7** in ethanol.

Dye	λ_{abs}[a] (nm)	ε (M-1 cm-1)	λ_{em}[b] (nm)	Φ_f[c] (%)	Stokes shift (nm)
Rho B	553	117000	572	53	19
RE1	628	93600	680	5.3	52
RE2	649	44000	716	< 3	67
RE3	604	94000	647	33	43
RE4	602	146400	665	10.8	63
RE5	618	43400	728	< 3	110
RE6	654	31000	745	< 3	91
RE7	677	22000	830	< 3	153

[a]Maximum absorption wavelength. [b]Maximum emission wavelength. [c]Relative fluorescence quantum yield estimated by using Nile Blue (Φ_f = 0.27 in ethanol) [13] as a fluorescence standard.

Biological imaging and cell location studies

NIR dyes are reportedly favorable for fluorescence imaging of living cells because NIR photons cause minimal photodamage to living cells and minimum interference from sample autofluorescence.[14] On the basis of the Φ_f values, we evaluated the potential utility of **RE1**, **RE3**, and **RE4** for bioimaging applications. First, costaining of HeLa cells with 4',6–diamidino–2–phenylindole (DAPI), **RE1**, **RE3**, and **RE4** led to obvious intracellular fluorescence (Fig. S2), indicating that the molecules were membrane-permeable. Some rhodamines[15] and Si-rhodamines[6b] reportedly localize in mitochondria owing to their lipophilic and cationic character. Therefore, we used **RE1**, **RE3**, and **RE4** for subcellular localization experiments involving colocalization of these dyes at a low concentration (50 nM) with various commercially available subcellular organelle markers. In images obtained with **RE1**, **RE3**, and **RE4**, the fluorescence of all three dyes

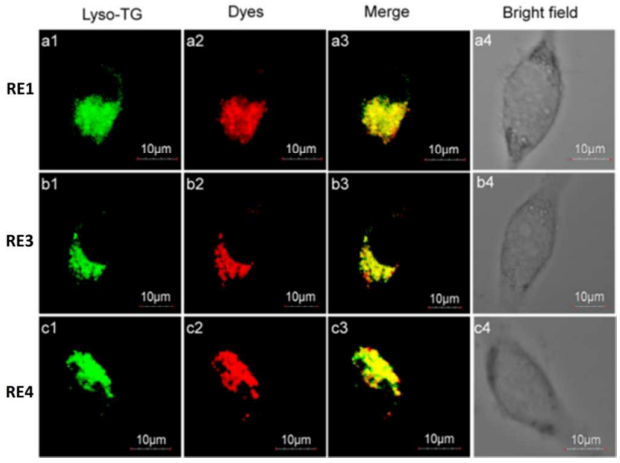

Fig. 3 Colocalization of **RE1**, **RE3**, and **RE4** (50 nM) with LysoTracker Green DND-26 (Lyso-TG) (200 nM) in L929 cells: (a1-c1) fluorescence images from Lyso-TG; (a2-c2) fluorescence images from **RE1**, **RE3**, and **RE4**, respectively; (a3-c3) merged images; and (a4-c4) bright-field images.

colocalized perfectly with that of LysoTracker Green DND-26 (the Pearson's coefficients were 0.94, 0.94 and 0.93, respectively; Fig. 3). In contrast, the fluorescence of the dyes did not colocalize with that of ER-Tracker Green, MitoTracker Green, or Golgi-Tracker Green (Fig. S3–S5). These findings demonstrate that **RE1**, **RE3**, and **RE4** accumulated specifically in the lysosomes. In an MTT ([3-(4,5-dimethylthiazol-2-yl)-2,5-diphenyl-2*H*-tetrazolium) assay, **RE1**, **RE3**, and **RE4** exhibited low cytotoxicity (cell viability >95%) at concentrations up to 250 nM after incubation with L929 cells, a murine aneuploid fibrosarcoma cell line, for 24 h (Fig. S6). Because the pH within lysosomes is in the 4.5–5.5 range, we evaluated the photostabilities[16] of **RE1**, **RE3**, **RE4**, **Rho B**, and Lyso-TG in phosphate-buffered saline (pH 5.5). After continuous irradiation for 2000 s, the fluorescence intensity of Lyso-TG had decreased to 93%, but little decrease in the emission intensities of **RE1**, **RE3**, **RE4**, and **Rho B** were observed (Fig. S7); this result indicates that **RE1**, **RE3**, and **RE4** retained the superior photostability of the parent xanthene dye. Under the

View Article Online
DOI: 10.1039/C8OB01701H

same conditions, **RE2**, **RE5**, and **RE6** all showed good photostabilities as well; no obvious decreases in fluorescence intensity were observed after 2000 s of irradiation (Fig. S7). Meanwhile, the photostabilities of **RE1**, **RE3**, **RE4**, and Lyso-TG were also investigated in cells. As shown in Fig. S8 and Videos S1-S4, dyes **RE1** and **RE4** possess superior photostability. However, the fluorescence signal intensity of **RE3** decayed gradually to 13% afer 30 min continuous irradiation and Lyso-TG became non-fluorescent only after 2 min.

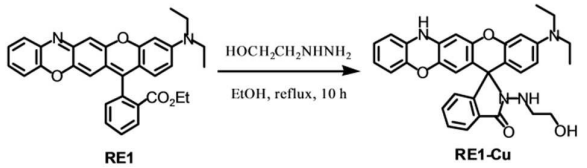

Scheme 4 Synthesis of the probe **RE1-Cu**.

Application of dye RE1 for designing fluorescent probe

Dyes **RE1-RE7** possess rhodamine-like spirolactam structure, which provides a universal platform for the design of efficient NIR turn-on bioimaging probes for various targets. To demonstrate the feasibility of this probe design, a NIR fluorescent probe, **RE1-Cu**, was synthesized for sensing Cu^{2+} by utilizing dye **RE1** as fluorophore and 2-hydroxyethylhydrazine unit as recognition unit (Scheme 4). Copper is the third-most abundant transition metal in the human body and plays a key role in a variety of fundamental physiological processes in organisms including enzyme functions and transcriptional events.[17] However, the disruption of copper homeostasis is closely connected with human genetic disorders like Wilson's[18] and Menkes disease;[19] neurodegenerative diseases such as Alzheimer's,[20] Parkinson's, and Huntington's[21] diseases. Therefore, the detection of copper in living systems is very important. [22]

Fig. 4 showed the spectroscopic properties of **RE1-Cu** at various Cu^{2+} concentrations in PBS buffer (0.01 M, pH 7.4, containing 25% CH_3CN as a cosolvent). No obvious absorption and fluorescence of **RE1-Cu** were observed because of its spirolactam form. The addition of Cu^{2+} ions elicited marked increases of absorption and fluorescence emission at 620 and 680 nm, respectively, along with an obvious change from colorless to blue. HRMS confirmed that the spectral changes of **RE1-Cu** were due to the Cu^{2+}-mediated ring-opening and spirolactam hydrolysis to form the fluorophore **RE1** (Fig. S9). The fluorescence turn-on constants ($K_{turn\text{-}on}$)[23] were estimated to be 10.67 ± 0.11 μM (R^2 = 0.997) by fluorescence titration (Fig. S10). The detection limit of the probe **RE1-Cu** for Cu^{2+} was evaluated to be 9.1 nM based on the signal-to-noise ratio of three method (Fig. S11), [24] which is much lower than the upper limit of cooper in drinking water defined by Administration of the People's Republic of China (ca. 15.7 μM) and U.S. Environmental Protection Agency (EPA) (ca. 20 μM). [25]

The time-dependent fluorescence response of the probe **RE1-Cu** towards Cu^{2+} ions was also measured. As shown in Fig. S12), the reaction between the probe and Cu^{2+} could complete in less than 2 min, which means that **RE1-Cu** can be used for the real-time detection of Cu^{2+}. In addtion, probe **RE1-Cu** exhibited good selectivity towards Cu^{2+} over other metal ions (Fig. S13a), and the competition experiment (Fig. S13b) revealed that all of the competitive metal ions had minor or no interference with the fluorescence response of **RE1-Cu** towards Cu^{2+}. Then, the fluorescence response of **RE1-Cu** to Cu^{2+} at different pH levels was explored and the results implied that the probe can be used for detecting Cu^{2+} in the pH range of 4 to 9, which meets the requirements for fluorescent tracers for use in biological applications (Fig. S14).

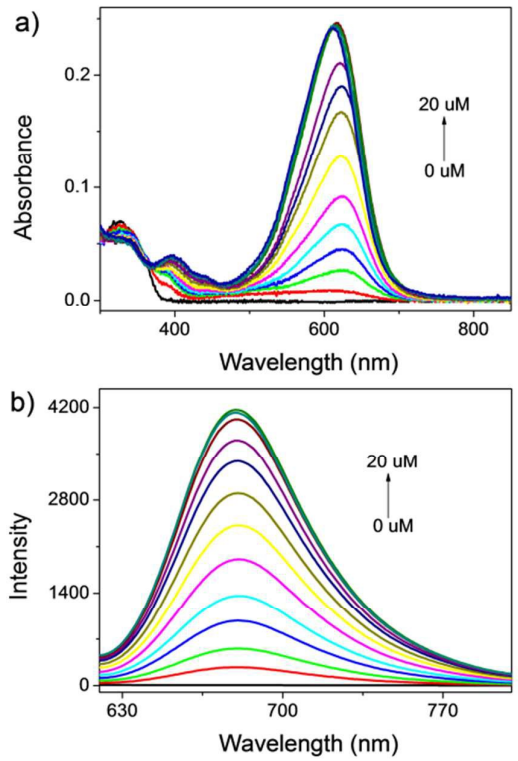

Fig. 4 a) Absorption and b) fluorescence spectra of **RE1-Cu** (5 μM) with different concentrations of Cu^{2+} in PBS buffer (0.01 M, pH 7.4, containing 25% CH_3CN as a cosolvent).

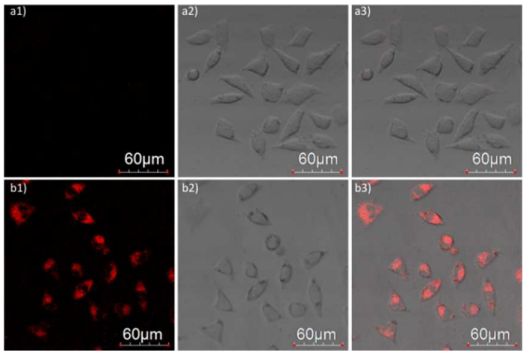

Fig. 5 Confocal fluorescence images of Cu^{2+} using **RE1-Cu** in L929 cells. (a1-a3) L929 cells were incubated with **RE1-Cu** (3 μM, 30 min) only; (b1-b3) L929 cells were pretreated with Cu^{2+} (10 μM, 30 min) and then were further incubated with **RE1-Cu** (3 μM) for 30 min. a1) and b1): fluorescence images; a2) and b2): bright-field images; a3) and b3) merged images.

View Article Online
DOI: 10.1039/C8OB01701H

The application of **RE1-Cu** for fluorescence imaging of Cu^{2+} in cultured living cells was demonstrated. L929 cells incubated with **RE1-Cu** (3 μM) for 30 min displayed almost no fluorescence (Fig. 5, a1-a3), which is consistent with the low brightness of **RE1-Cu** in aqueous solutions. In the presence of Cu^{2+}, probe-loaded L929 cells showed bright red fluorescence (Fig. 5, b1-b3), which means that **RE1-Cu** is cell membrane permeable and can be used for detecting Cu^{2+} in living cells.

Conclusions

In summary, we synthesized a series of heterocyclic fused π-extended rhodamine dyes (**RE1–RE7**) with rectilinearly arranged fused aromatic rings. The dyes were synthesized via an intramolecular S_NAr^H reaction to cyclize heterocyclic rings to the benzene ring of preorganized 2-aminoaryl linked xanthylium under mild conditions without a transition metal catalyst under mild conditions. The emission maxima of **RE1–RE7** were significantly red-shifted (to the NIR region) relative to the corresponding maxima for traditional rhodamine dyes and **RE1**, **RE3**, and **RE4** could be utilized for lysosome labeling. Furthermore, a NIR fluorescent probe, **RE1-Cu** for Cu^{2+}, was synthesized using **RE1** as a platform, and successfully applied for the imaging of Cu^{2+} in living cells, demonstrating the potential bioimaging applications of the new probe. We expect the synthesis strategy that used in our text can be extended to the preparation of a wide variety of heterocyclic fused π-extended NIR rhodamine dyes.

Experimental

Additional schemes, UV/Vis and fluorescence spectra figures; subcellular localization and cytotoxicity experiment procedures, and confocal microscopy fluorescence imaging; experimental procedures for synthesis of dyes **RE1**-**RE7** and probe **RE1-Cu**, ^1H, ^{13}C NMR and HRMS spectra for new compounds are included in the Supporting Information. The photostabilites of dyes **RE1**, **RE3**, **RE4** and Lysotracker green in L929 were recorded in videos S1-S4 (AVI).

CCDC 1582793 (dye **RE1**) contains the supplementary crystallographic data for this paper. These data are provided free of charge by The Cambridge Crystallographic Data Centre.

Conflicts of interest

There are no conflicts to declare.

Acknowledgements

We gratefully acknowledge the Natural Science Foundation of China (NNSFC 21272172), and the Scientific Developing Foundation of Tianjin Education Commission (2017ZD14).

Notes and references

1 (a) Z. Guo, S. Park, J. Yoon and I. Shin, *Chem. Soc. Rev.*, 2014, **43**, 16; (b) E. L. Que, D. W. Domaille and C. J. Chang, *Chem. Rev.*, 2008, **108**, 1517.

2 (a) X. Chen, T. Pradhan, F. Wang, J. S. Kim and J. Yoon, *Chem. Rev.*, 2012, **112**, 1910; (b) D. L. Ma, D. S. H. Chan and C. H. Leung, *Acc. Chem. Res.*, 2014, **47**, 3614; (c) M. Beija, C. A. M. Afonsoa and J. M. G. Martinhoa, *Chem. Soc. Rev.*, 2009, **38**, 2410-2433; (d) C. Liu, C. Yang, L. Lu, W. Wang, W. Tan, C.-H. Leung and D.-L. Ma, *Chem. Commun.*, 2017, **53**, 2822; (e) Z. Yang, M. She, S. Ma, B. Yin, P. Liu, X. Liu, S. Zhao and J. Li, *Sens. Actuators B: Chem.,* 2017, **242**, 872; (f) C. Liu, X. Jiao, Q. Wang, K. Huang, S. He, L. Zhao, X. Zeng, *Chem. Commun.* 2017, **53**, 10727; (g) Z. Mao, M. Wang, J. Liu, L.-J. Liu, S. M.-Y. Lee, C.-H. Leung and D.-L. Ma, *Chem. Commun.*, 2016, **52**, 4450; (h) P. Nandhikonda, S. Paudel and M. D. Heagy, *Tetrahedron*, 2009, **65**, 2173.

3 (a) N. Karton-Lifshin, E. Segal, L. Omer, M. Portnoy, R. Satchi-Fainaro and D. Shabat, *J. Am. Chem. Soc.*, 2011, **133**, 10960; (b) J. M. Baumes, J. J. Gassensmith, J. Giblin, J.-J. Lee, A. G. White, W. J. Culligan, W. M. Leevy, M. Kuno and B. D. Smith, *Nat. Chem.*, 2010, **2**, 1025.

4 (a) Y. Liu, J. Zhou, L. Wang, X. Hu, X. Liu, M. Liu, Z. Cao, D. Shangguan and W. Tan, *J. Am. Chem. Soc.*, 2016, **138**, 12368. (b) M. Ogawa, N. Kosaka, P. L. Choyke and H. Kobayashi, *Cancer Res.*, 2009, **69**, 1268; (c) W. Sun, S. Guo, C. Hu, J. Fan and X. Peng, *Chem. Rev.*, 2016, **116**, 7768.

5 (a) M. E. Sanborn, B. K. Connolly, K. Gurunathan and M. Levitus, *J. Phys. Chem. B,* 2007, **111**, 11064; (b) K. Jia, Y. Wan, A. Xia, S. Li, F. Gong and G. Yang, *J. Phys. Chem. A*, 2007, **111**, 1593.

6 (a) M. Fu, Y. Xiao, X. Qian, D. Zhao and Y. Xu, *Chem. Commun.*, 2008, 1780; (b) Y. Koide, Y. Urano, K. Hanaoka, T. Terai and T. Nagano, *ACS Chem. Biol.*, 2011, **6**, 600; (c) Y. Koide, Y. Urano, K. Hanaoka, W. Piao, M. Kusakabe, N. Saito, T. Terai, T. Okabe and T. Nagano, *J. Am. Chem. Soc.*, 2012, **134**, 5029.

7 (a) T. F. Brewer and C. J. Chang, *J. Am. Chem. Soc.,* 2015, **137**, 10886; (b) T. Egawa, K. Hanaoka, Y. Koide, S. Ujita, N. Takahashi, Y. Ikegaya, N. Matsuki, T. Terai, T. Ueno, T. Komatsu and T. Nagano, *J. Am. Chem. Soc.*, 2011, **133**, 14157; (c) A. N. Butkevich, Y, G. Mitronova, S. C. Sidenstein, J. L. Klocke, D. Kamin, D. N. H. Meineke, E. D'Este, P.-T. Kraemer, J. G. Danzl, V. N. Belov and S. W. Hell, *Angew. Chem., Int. Ed.*, 2016, **55**, 3290; (d) P. Shieh, M. S. Siegrist, A. J. Cullen and C. R. Bertozzi, *PNAS*, 2014, **111**, 5456; (e) S. Uno, M. Kamiya, T. Yoshihara, K. Sugawara, K. Okabe, M. C. Tarhan, H. Fujita, T. Funatsu, Y. Okada, S. Tobita and Y. Urano, *Nat. Chem.*, 2014, **6**, 681; (f) A. Roth, H. Li, C. Anorma and J. Chan, *J. Am. Chem. Soc.*, 2015, **137**, 10890.

8 (a) M. Sibrian-Vazquez, J. O. Escobedo, M. Lowry, F. R. Fronczek and R. M. Strongin, *J. Am. Chem. Soc.*, 2012, **134**, 10502; (b) Y. Yang, M. Lowry, X. Xu, J. O. Escobedo, M. Sibrian-Vazquez, L. Wong, C. M. Schowalter, T. J. Jensen, F. R. Fronczek, I. M. Warner and R. M. Strongin, *PNAS*, 2008, **105**, 8829.

9 Q. A. Best, A. E. Johnson, B. Prasai, A. Rouillere and R. L. McCarley, *ACS Chem. Biol.*, 2016, **11**, 231.

10 (a) K. Błaziak, W. Danikiewicz and M. Mąkosza, *J. Am. Chem. Soc.,* 2016, **138**, 7276; (b) M. Mąkosza, *Chem. Soc. Rev.,* 2010, **39,** 2855; (c) M. Mąkosza and K. Wojciechowski, *Chem. Rev.,* 2004, **104**, 2631; (d) M. Mąkosza, *Chem. -Eur. J.,* 2014, **20**, 5536.

11 (a) T. Peng and D. Yang, *Org. Lett.,* 2010, **12**, 496; (b) G. Evano, N. Blanchard and M. Toumi, *Chem. Rev.,* 2008, **108**, 3054; (c) J. Bariwal and E. Van der Eycken, *Chem. Soc. Rev.,* 2013, **42**, 9283; (d) F. Ullmann, *Ber. Dtsch. Chem. Ges.,* 1903, **36**, 2382.

View Article Online
DOI: 10.1039/C8OB01701H

12 (a) W. Xiao, Z. He, S. Remiro-Buenamañana, R. J. Turner, M. Xu, X. Yang, X. Jing and A. N. Cammidge, *Org. Lett*., 2015, **17**, 3286; (b) R. Sun, W. Liu, Y.-J. Xu, J.-M. Lu, J.-F. Ge and M. Ihara, *Chem. Commun.*, 2013, **49**, 10709.
13 R. Sens, K. H. Drexhage, *J. Luminesc.*, 1981, **24**, 709.
14 H. Kobayashi, M. Ogawa, R. Alford, P. L. Choyke and Y. Urano, *Chem. Rev.*, 2010, **110**, 2620.
15 P. Haugland, The Handbook: A Guide to Fluorescent Probes and Labeling Technologies, 10th ed.. Molecular Probes, Eugene, OR, 2005.
16 X. Zhou, R. Lai, J. R. Beck, H. Li and C. I. Stains, *Chem. Commun.*, 2016, **52**, 12290.
17 (a) R. Uauy, M. Olivares and M. Gonzalez, *Am. J. Clin. Nutr.,* 1998, **67**, 952S; (b) I. H. Scheinberg and I. Sternlieb, *Am. J. Clin. Nutr.,* 1996, **63**, 842S.
18 (a) S. Lutsenko, A. Gupta, J. L. Burkhead and V. Zuzel, *Arch. Biochem. Biophys*., 2008, **476**, 22; (b) S. Lutsenko, *Biochem. Soc. Trans.,* 2008, **36**, 1233; (c) D. Huster, M. Hoppert, S. Lutsenko, J. Zinke, C. Lehmann, J. Mossner, F. Berr and K. Caca, *Gastroenterology,* 2003, **124**, 335.
19 (a) S. Sisodiya, *Nat. Rev. Neurol.*, 2011, **7**, 129; (b) C. Vulpe, B. Levinson, S. Whitney, S. Packman and J. Gitschier, *Nat. Genet.,* 1993, **3**, 7; (c) S. G. Kaler, *Nat. Rev. Neurol.,* 2011, **7**, 15; (d) S. La Fontaine and J. F. Mercer, *Arch. Biochem. Biophys.*, 2007, **463**, 149.
20 (a) S. Ayton, P. Lei and A. I. Bush, *Free Radical Biol. Med.,* 2013, **62**, 76; (b) K. J. Barnham, C. L. Masters and A. I. Bush, *Nat. Rev. Drug Discovery,* 2004, **3**, 205; (c) M. G. Savelieff, S. Lee, Y. Liu and M. H. Lim, *ACS Chem. Biol.,* 2013, **8**, 856; (d) K. E. Matlack, D. F. Tardiff, P. Narayan, S. Hamamichi, K. A. Caldwell, G. A. Caldwell and S. Lindquist, *Proc. Natl. Acad. Sci. U. S. A.,* 2014, **111**, 4013.
21 G. Xiao, Q. Fan, X. Wang and B. Zhou, Proc. *Natl. Acad. Sci. U. S. A.,* 2013, **110**, 14995.
22 (a) Z. Yang, M. She, J. Zhang, X. Chen, Y. Huang, H. Zhu, P. Liu, J. Li and Z. Shi, *Sens. Actuators B: Chem.,* 2013, **176**, 482; (b) M. She, Z. Yang, L. Hao, Z. Wang, T. Luo, M. Obst, P. Liu, Y. Shen, S. Zhang and J. Li, *Sci. Rep.,* 2016, **6**, 28972; (c) F. Yu, W. Zhang, P. Li, Y. Xing, L. Tong, J. Ma and B. Tang, *Analyst*, 2009, **134**, 1826.
23 (a) P. Du and S. J. Lippard, *Inorg. Chem.,* 2010, **49**, 10753; (b) F. Yu, X. Han and L. Chen, *Chem. Commun.,* 2014, **50**, 1223.
24 M.-Z. Tian, M.-M. Hu, J.-L. Fan, X.-J. Peng, J.-Y. Wang, S.-G. Sun and R. Zhang, *Bioorg. Med. Chem. Lett.,* 2013, **23**, 2916.
25 H. S. Jung, P. S. Kwon, J. W. Lee, J. I. Kim, C. S. Hong, J. W. Kim, S. Yan, J. Y. Lee, J. H. Lee, T. Joo and J. S. Kim, *J. Am. Chem. Soc.,* 2009, **131**, 2008.
26 (a) E. Azuma, N. Nakamura, K. Kuramochi, T. Sasamori, N. Tokitoh, I. Sagami and K. Tsubaki, *J. Org. Chem.,* 2012, **77**, 3492; (b) J. Qin, H. Yao, S. He, X. Zeng, *RSC Adv.* 2016, **6**, 75570; (c) M. Sibrian-Vazquez, J. O. Escobedo, M. Lowry, F. R. Fronczek and R. M. Strongin, *J. Am. Chem. Soc.,* 2012, **134**, 10502; (d) Q. Wang, X. Jiao, C. Liu, S. He, L. Zhao and X. Zeng, *J. Mater. Chem. B*, 2018, **6**, 4096.